

Original Article

IGLL5 has potential to be a prognostic biomarker and its correlation with immune infiltrates in breast cancer

Junchao Feng^{1*}, Yuhan Hou^{1*}, Chang Liu^{2*}, Youyou Wang¹, Weibo Chen¹, Yulong Liu², Huahui Bian¹

¹Department of Nuclear Accident Medical Emergency, The Second Affiliated Hospital of Soochow University, Suzhou 215004, Jiangsu, China; ²Clinical Diagnosis and Treatment Center of Oncology, The Second Affiliated Hospital of Soochow University, Suzhou 215004, Jiangsu, China. *Equal contributors.

Received March 29, 2025; Accepted May 17, 2025; Epub June 15, 2025; Published June 30, 2025

Abstract: Background: The tumor microenvironment (TME) of breast cancer (BRCA) influences disease progression through dynamic interactions between immunity and stroma, but its key regulatory molecules and prognostic value remain to be elucidated. The aim of this study was to explore the prognostic potential of immunoglobulin λ -like polypeptide 5 (IGLL5) in BRCA and its association with immune infiltration in TME. Methods: 1178 BRCA cases were obtained from The Cancer Genome Atlas (TCGA) database. CIBERSORT and ESTIMATE computational methods were used to quantify the composition of tumor-infiltrating immune cells (TICs) and the presence of immune and stromal components. Prognostic indicator closely associated with BRCA was identified by Cox regression analysis and protein-protein interaction (PPI) network construction. Through Gene Set Enrichment Analysis (GSEA) and other means, the correlations between IGLL5 expression and patient survival, immune activities, metabolic pathways, and immune cell types were studied. Results: Overall survival was significantly prolonged in patients with high IGLL5 expression (HR=0.62, 95% CI 0.45-0.86, $P=0.013$) and positively correlated with immune-activating pathways (complement signaling, interferon response) and anti-tumor TICs (CD8⁺ T cells, M1 macrophages) ($r>0.3$, $P<0.001$) and negatively correlated with tumor-promoting TICs (M2 macrophages, resting NK cells). The low IGLL5 group was enriched in metabolic pathways (estrogen response, oxidative phosphorylation), suggesting that it may promote immune escape through metabolic reprogramming. Conclusion: IGLL5 is a novel prognostic marker for BRCA, and its expression level affects patient survival by modulating TME immune infiltration and metabolic reprogramming. This study provides a theoretical basis for IGLL5-directed immunotherapeutic strategies (e.g., combining PD-1 inhibitors), and its mechanism needs to be verified by multicenter clinical cohorts and functional experiments in the future.

Keywords: IGLL5, tumor microenvironment, immune infiltration, breast cancer, prognostic

Introduction

Breast Cancer (BRCA), the most common malignant tumor among female patients worldwide, accounted for 11.6% of all newly diagnosed cancer cases globally in 2022, resulting in 665,684 deaths and continuing to grow at a rate of approximately 0.6% per year [1, 2]. Currently, the treatment of BRCA includes surgical resection, chemotherapy, radiotherapy, and targeted therapy. Although the five-year survival rate of BRCA has been greatly improved with the development of technology, some patients will have a poor prognosis due to delayed diagnosis, metastasis and other factors [3-5]. Consequently, there is an urgent need to

find effective markers for early diagnosis, prognosis and treatment of BRCA.

The tumor microenvironment (TME), an important part of the tumor mass, which consists of tumor cells, fibroblasts, immune and inflammatory cells, stromal cells, intercellular matrix, microvessels, and biological molecules that infiltrate them [6, 7]. Emerging evidence highlights the TME as a critical orchestrator in the pathogenesis of bladder cancer and glioblastoma [8, 9]. Tumor-infiltrating immune cells (TICs) within the TME are crucial for tumor diagnosis, determining clinical treatment sensitivity, and influencing patient survival outcomes [10]. The stromal cells and immune cells in the TME are

involved in the tumor progression [11]. Previous studies have shown that TME score has a high sensitivity in predicting the efficacy of immunotherapy in gastric cancer [8, 12]. TME acts as a complex ecosystem, which could support tumor growth as well as metastasis while attenuating immunosurveillance [7, 13-15]. TME has recently emerged as an important player in BRCA progression and could be a future therapeutic target [7]. Currently, BRCA is considered an immunogenic and vascularized tumor. Several studies have found that the immune cells infiltrated in the TME block the effective antitumor response [16]. Nevertheless, the specific regulatory mechanism of the role of the TME in BRCA remains unclear. Therefore, a comprehensive understanding of the characteristics of the TME is urgently needed to improve the immunotherapy.

In the current study, we used ESTIMATE and CIBERSORT computational methods to determine the proportion of TICs and the ratio of immune and stromal components in BRCA samples sourced from The Cancer Genome Atlas (TCGA) database. Moreover, we have uncovered that immunoglobulin lambda-like polypeptide 5 (IGLL5) may serve as a potential indicator for the alteration of TME status in BRCA, this will provide valuable evidence for clinical diagnosis and treatment decisions.

Materials and methods

Raw data acquisition

We retrieved RNA sequencing (RNA-seq) transcriptomic profiles of 1,178 BRCA cases from TCGA database (<https://portal.gdc.cancer.gov/>), comprising 99 normal tissue specimens and 1,079 tumor samples [17, 18]. Additionally, we acquired comprehensive clinical annotations from the TCGA portal, including tumor staging parameters, TNM classification criteria, overall survival records, and prognostic metadata.

Analysis of ImmuneScore, StromalScore and ESTIMATEScore

Based on the gene expression data of the TCGA-BRCA cohort, the R package estimation algorithm was used to calculate the ImmuneScore, StromalScore, and ESTIMATEScore. All

BRCA samples were divided into high and low groups according to the median values of each score (ImmuneScore, StromalScore, EstimatScore). Higher scores in ImmuneScore or StromalScore indicate a greater abundance of immune or stromal components in the TME, respectively. ESTIMATEScore, derived by summing ImmuneScore and StromalScore, represents the combined proportion of both components in the TME.

Survival analysis

We conducted survival analysis by R language packages [19]. We employed the Kaplan-Meier method to analyze 1079 tumor samples and plotted survival curves. Furthermore, we used the log-rank test to further evaluate the differences in survival outcomes.

DEGs between high and low groups

We performed differentially expressed genes (DEGs) using the limma package on 1,079 tumor samples that were stratified into high and low groups, with genes demonstrating an absolute log₂ fold change >1 and false discovery rate (FDR)-adjusted $P < 0.05$ considered statistically significant. Subsequently, we employed the pheatmap R package to generate hierarchical clustering heatmaps after log₂ transformation of expression values, effectively visualizing distinct expression patterns of DEGs across the stratified sample groups.

GO and KEGG enrichment analysis

We performed systematic Gene Ontology (GO) and Kyoto Encyclopedia of Genes and Genomes (KEGG) pathway enrichment analysis on the identified DEGs using the clusterProfiler package in R [20]. The analysis workflow incorporated complementary visualization tools from enrichplot and ggplot2 packages for comprehensive results interpretation. Statistically significant functional terms and biological pathways were selected using dual criteria of nominal significance ($p < 0.05$) and multiple testing correction ($q < 0.05$), ensuring robust identification of biologically relevant patterns.

Difference analysis of clinical stages

Clinicopathological data for BRCA samples were retrieved from TCGA. Statistical analyzes

were systematically conducted using Wilcoxon rank-sum tests (two-group comparisons) and Kruskal-Wallis tests (multi-group comparisons) to evaluate molecular profile disparities across clinical stages. These analyzes revealed significant associations between molecular signatures and disease progression parameters.

PPI network construction

Protein-Protein Interaction (PPI) network was generated using the STRING database and subsequently optimized in Cytoscape (v3.10.0). A high-stringency confidence threshold (interaction score >0.95) was applied to filter spurious associations, yielding a core network of biochemically validated interactions. Network topology analysis focused on hub proteins demonstrating >5 functional connections.

COX regression analysis

Univariate Cox proportional hazards regression was implemented via the survival R package to identify progression-relevant genes. Top prognostic candidates were selected for downstream validation, with effect sizes and confidence intervals visualized through multivariable-adjusted forest plots.

Gene set enrichment analysis

Hallmark and C7 immunologic gene sets (MSigDB v6.2) were analyzed using clusterProfiler with Gene Set Enrichment Analysis (GSEA) methodology. Pathway activation states were quantified via GSVA scores across the tumor cohort. Significant enrichments were defined by dual thresholds (NOM $p < 0.05$, FDR $q < 0.06$), with leading-edge analysis identifying core contributing genes.

TICs profile

The CIBERSORT computational method was utilized to estimate the TICs abundance profile in all tumor samples. Subsequently, a quality filtering step was implemented, where only tumor samples with a $P < 0.05$ were retained for further analysis. This rigorous selection criterion ensured that only samples with reliable estimations of immune cell abundance were included in the subsequent analysis, enhancing the robustness and accuracy of the findings

related to the tumor immune microenvironment.

Statistical methods

The statistical analysis of the data will be conducted using the default statistical analysis methods provided by the databases. For the comparison of IGLL5 expression levels between cancer tissues and normal tissues, the Wilcoxon test will be used for the comparison of IGLL5 expression levels between BRCA and normal tissues, one-way analysis of variance will be employed. For the comparison of survival rates between high IGLL5 expression and low IGLL5 expression, the Logrank test will be used. A significance level of $P < 0.05$ will be considered statistically significant for differences.

Results

Analysis process of the present study

Transcriptomic RNA sequencing data from 1178 BRCA cases were obtained from the TCGA database. ImmuneScore and StromalScore were calculated using the ESTIMATE algorithm to quantify TME characteristics. Subsequently, immune/stromal score-based DEGs were screened, followed by construction of a PPI network through the STRING database. Univariate Cox regression analysis with Benjamini-Hochberg correction identified IGLL5, KLRB1, CCL19, CD3E, and CD40LG as hub genes. Survival analysis showed that IGLL5 had a significant impact on the prognosis of BRCA. Besides, we conducted Cox regression analysis to more accurately evaluate the independent prognostic value of IGLL5, used GSEA technology to explore the potential biological pathways associated with IGLL5, and also analyzed the correlation between IGLL5 and TICs to understand its role in TME. The analysis process is shown in **Figure 1**.

Analysis of ImmuneScore, StromalScore and ESTIMATEScore

As shown in **Figure 2A**, we found the higher the ImmuneScore, the higher the survival rate ($P < 0.05$). In contrast, as shown in **Figure 2B** and **2C**, neither the StromalScore nor the ESTIMATEScore is significantly correlated with

IGLL5 as indicator for BRCA

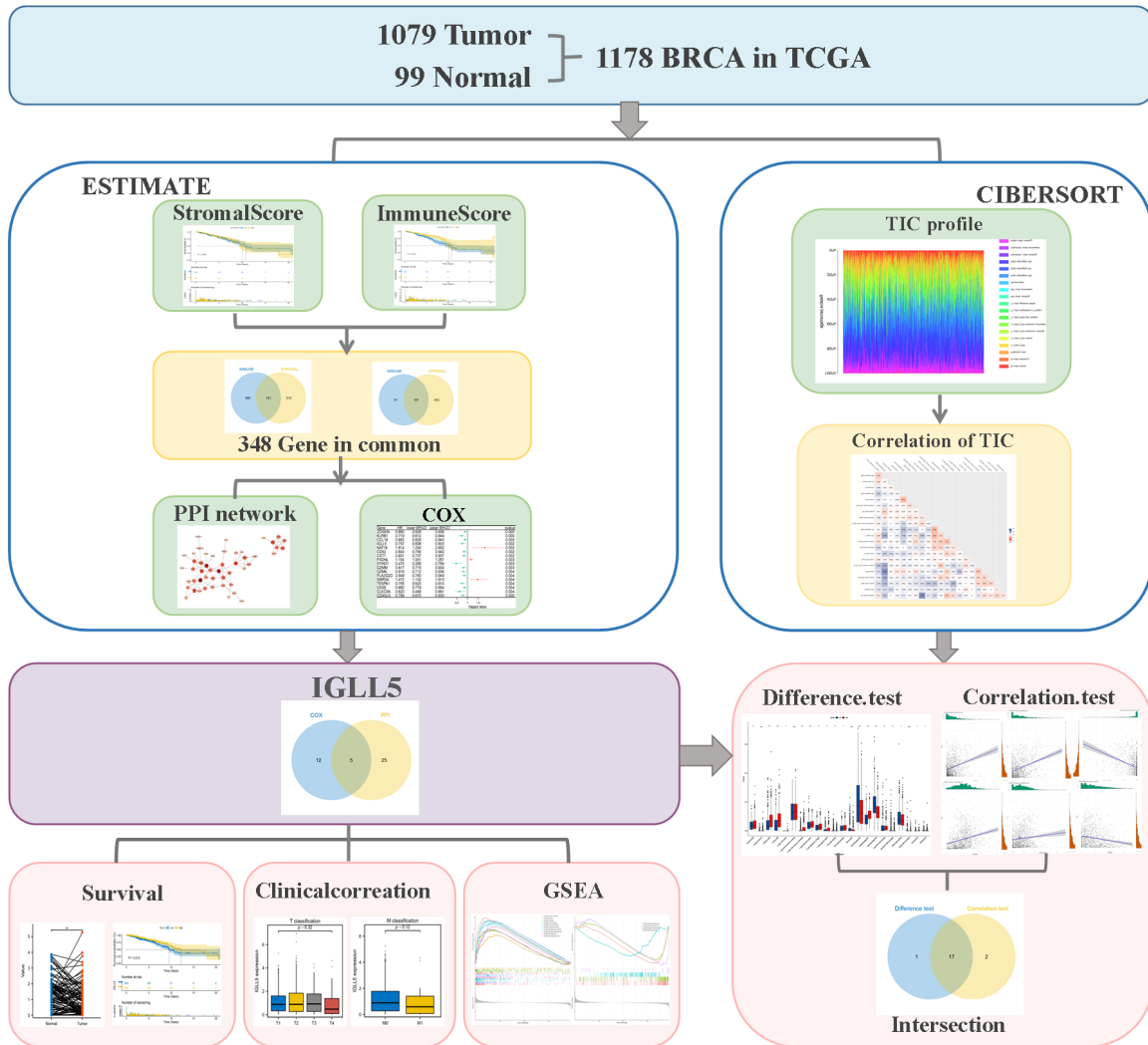


Figure 1. Analysis workflow of this study.

the overall survival rate. In addition, we found that the ImmuneScore, StromaScore, and ESTIMATEScore are not significantly correlated with the TNM stage, as shown in **Figure 3**.

Gene profile and functional enrichment analysis

We identified 1,124 DEGs through comparative analysis of high and low groups, with 876 genes upregulated and 248 genes downregulated (**Figure 4A, 4B**). Similarly, stromal core analysis revealed 1,291 DEGs, including 701 upregulated genes and 590 downregulated genes (**Figure 4A, 4B**). The Venn plot intersection analysis demonstrated 191 commonly upregulated genes and 153 commonly downregulated genes shared between the ImmuneScore and

StromaScore groups, yielding a total of 348 screened genes. Additionally, GO enrichment analysis identified critical pathways such as somatic recombination of immune receptors constructed from immunoglobulin superfamily domains and adaptive immune responses mediated by leukocytes (**Figure 4C**). KEGG enrichment analysis highlighted enriched pathways, including cytokine-cytokine receptor interaction, primary immunodeficiency, and viral protein interaction with cytokines and cytokine receptors (**Figure 4D**).

Intersection analysis of PPI network and univariate COX regression

We revealed a comprehensive interactome containing 348 candidate genes (**Figure 5A**).

IGLL5 as indicator for BRCA

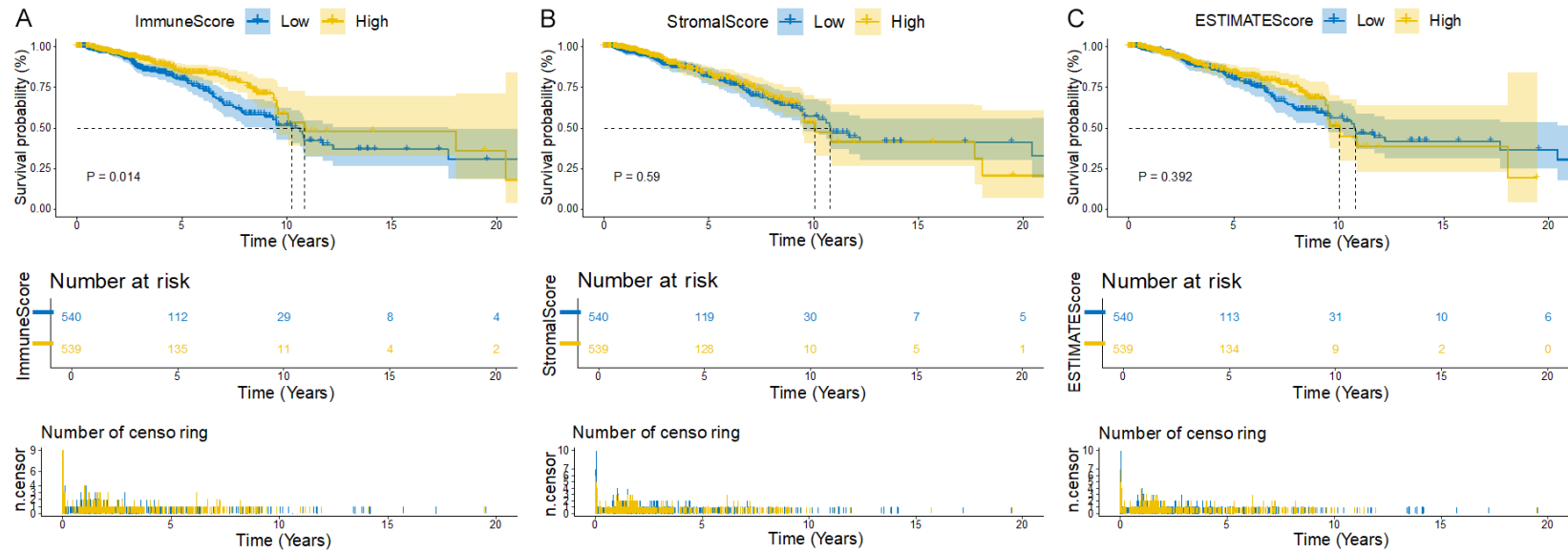


Figure 2. Correlation of scores with the survival of patients with BRCA. A. Kaplan-Meier survival analysis for BRCA patients divided by ImmuneScore into high or low groups ($P=0.014$, log-rank test). B. Kaplan-Meier survival analysis for BRCA patients divided by StromalScore into high or low groups ($P=0.59$, log-rank test). C. Kaplan-Meier survival analysis for BRCA patients with high and low ESTIMATEScore ($P=0.392$, log-rank test).

IGLL5 as indicator for BRCA

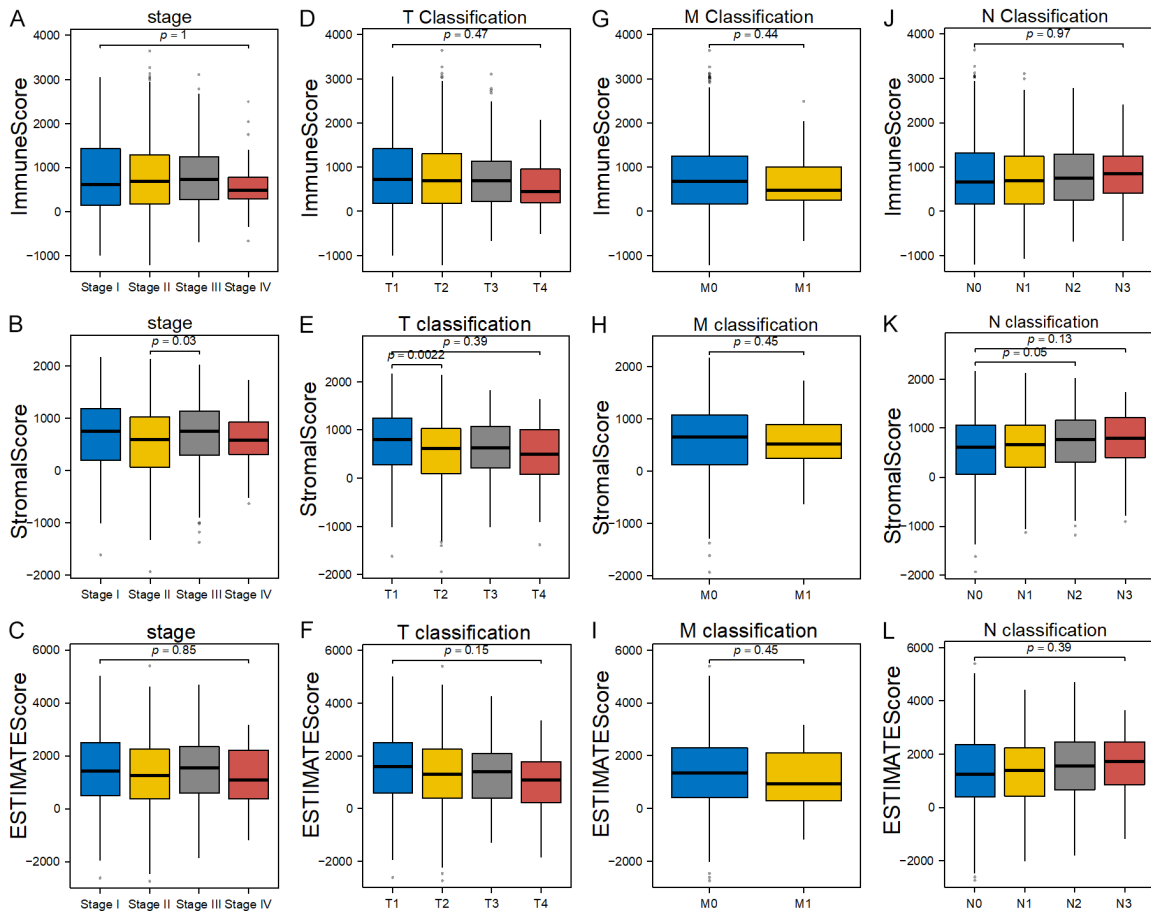


Figure 3. Correlation of scores with clinicopathological staging characteristics. A-C. Distribution of ImmuneScore, StromalScore, and ESTIMATEScore in stage. D-F. Distribution of ImmuneScore, StromalScore, and ESTIMATEScore in T classification. G-I. Distribution of ImmuneScore, StromalScore, and ESTIMATEScore in M classification. J-L. Distribution of ImmuneScore, StromalScore, and ESTIMATEScore in N classification.

Moreover, node connectivity analysis identified the top 30 hub proteins ranked by degree centrality (**Figure 5B**). Furthermore, univariate Cox proportional identified 17 survival-associated genes (\log -rank $p < 0.05$) visualized in a multivariable-adjusted forest plot (**Figure 5C**). Thereafter, integrative analysis intersecting the top network hubs (degree-ranked top 30) and survival-significant genes yielded five consensus biomarkers, including IGLL5, KLRB1, CC-L19, CD3E, and CD40LG (**Figure 5D**).

The correlation of IGLL5 expression with the survival and TNM stages

In this study, we found BRCA patients with high IGLL5 expression exhibited longer overall survival (**Figure 6C**). Furthermore, the Wilcoxon rank sum test demonstrated that the expres-

sion of IGLL5 in tumor samples and paired samples was significantly lower than that in normal samples (**Figure 6A, 6B**). However, there was no significant correlation between IGLL5 expression and the TNM stage of BRCA (**Figure 6D-G**).

GSEA enrichment analysis

We conducted GSEA and found that genes in the high IGLL5 expression group were predominantly enriched in immune-related activities, such as allograft rejection, complement signaling, interleukin signaling, and interferon response (**Figure 7A**). Conversely, genes in the low IGLL5 expression group were enriched in metabolic pathways, including estrogen response, oxidative phosphorylation, and pancreas β cells (**Figure 7B**). Additionally, immune-related gene

IGLL5 as indicator for BRCA

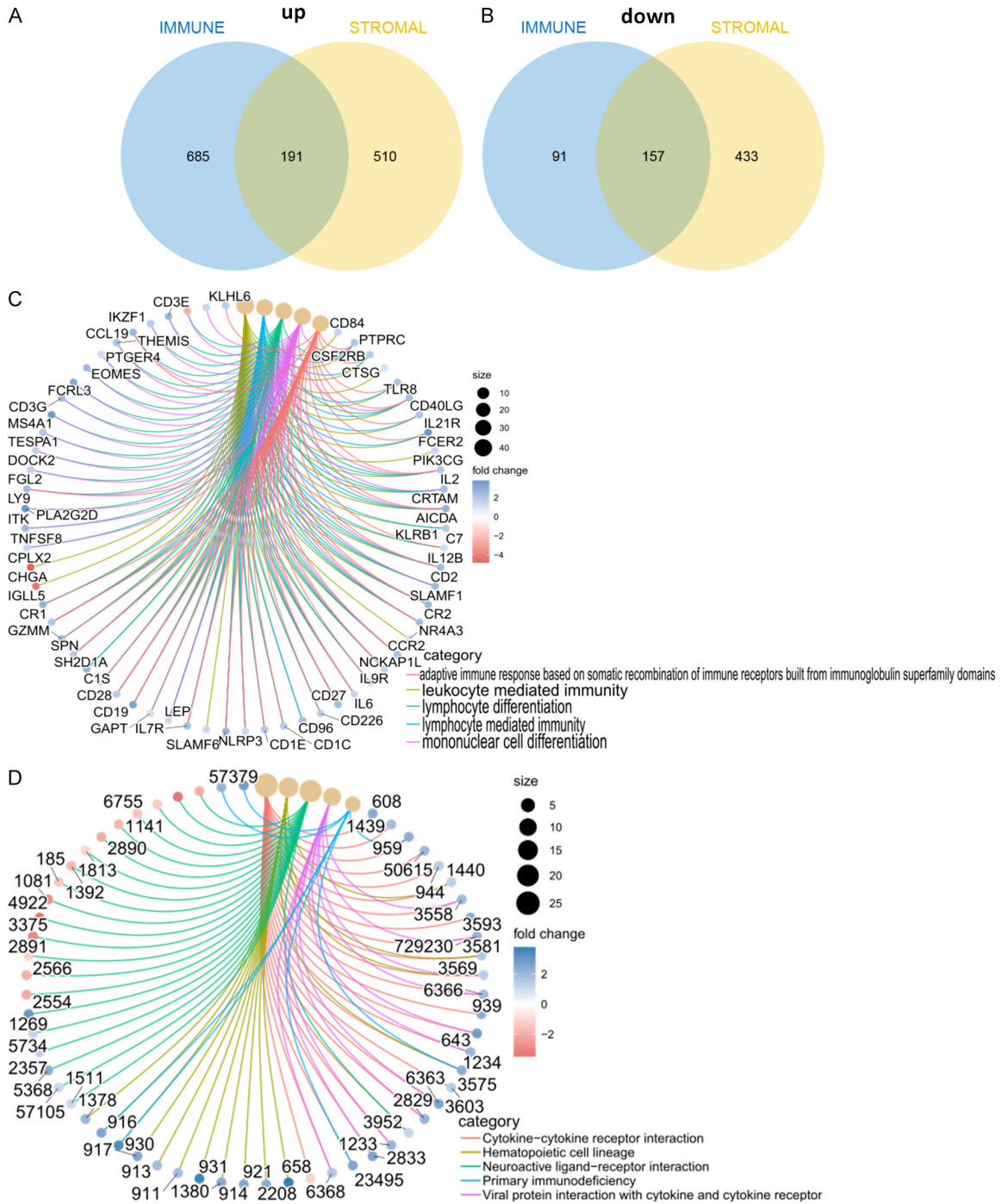


Figure 4. Screening of DEGs and enrichment analysis of GO and KEGG. A, B. Venn plots showing common up-regulated and down-regulated DEGs shared by ImmuneScore and StromalScore. C, D. GO and KEGG enrichment analysis for 379 DEGs, terms with p and $q < 0.05$ were considered to be enriched significantly.

sets were significantly enriched in the high IGLL5 expression group, encompassing pathways associated with B cells, CD4⁺ T cells, and NK T cells (**Figure 7C**). Nevertheless, a limited number of gene sets showed enrichment in the low IGLL5 expression group (**Figure 7D**).

Correlation of IGLL5 with the proportion of TICs

We analyzed the proportion of TIC subsets in BRCA samples using the CIBERSORT algorithm, constructing immune cell profiles for 21

IGLL5 as indicator for BRCA

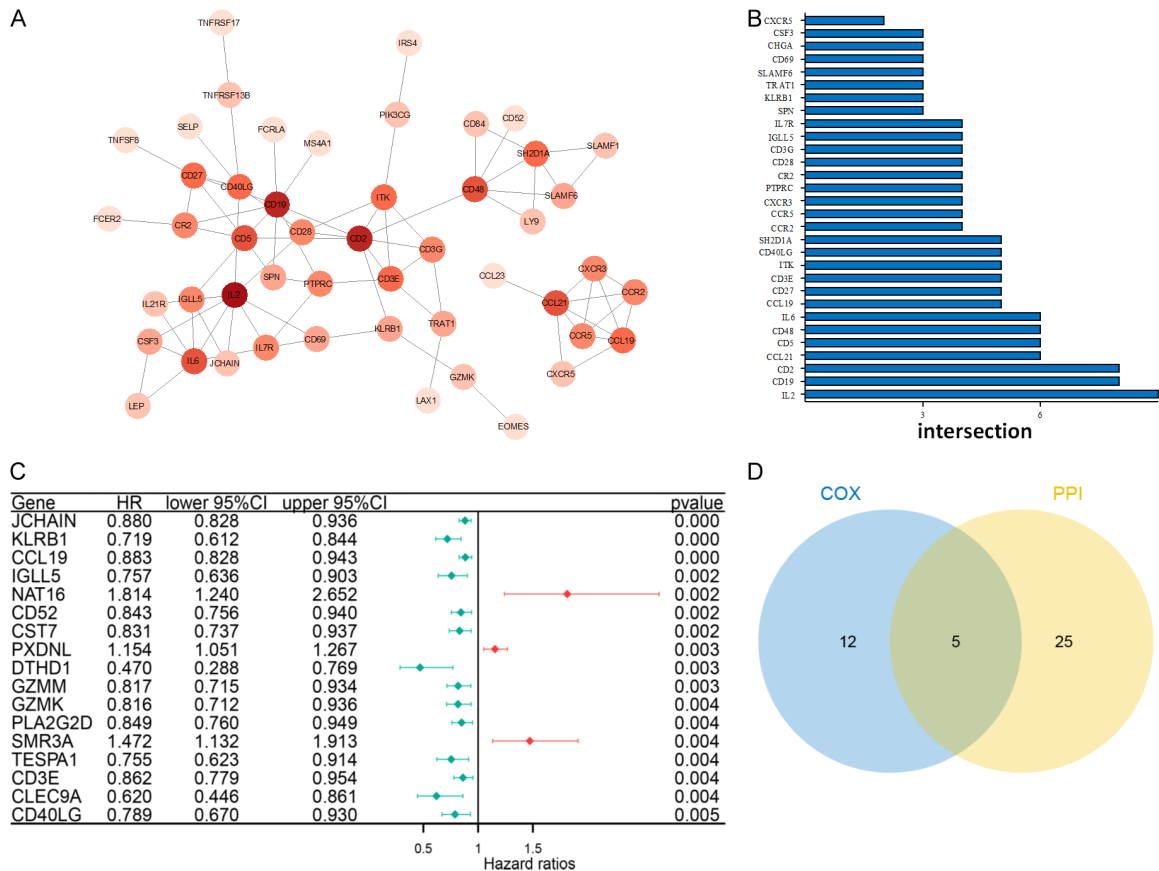


Figure 5. PPI network and univariate COX analysis. A. Interaction network constructed with the nodes with interaction confidence value >0.95. B. The top 30 genes ordered by the number of nodes. C. Univariate COX regression analysis with 379 DEGs, listing the top significant genes with $P < 0.005$. D. Venn plot showing the common genes shared by leading 30 nodes in PPI and top significant genes in univariate COX.

distinct immune cell types (**Figure 8**). The results from the difference and correlation analysis revealed that a total of 17 TICs types were correlated with the expression of IGLL5 (**Figure 9B, 9C**). Among these TICs, the expression of IGLL5 demonstrated positive correlations with 9 types of TICs, including naive B cells, plasma cells, CD8⁺ T cells, naive CD4⁺ T cells, activated CD4⁺ memory T cells, follicular helper T cells, regulatory T cells, gamma delta T cells, and M1 macrophages (**Figure 9A**). Conversely, 8 TIC types exhibited negative correlations with IGLL5 expression, comprising resting NK cells, M0 macrophages, M2 macrophages, resting dendritic cells, activated dendritic cells, resting mast cells, eosinophils, and neutrophils (**Figure 9A**).

Discussion

BRCA is one of the most common malignancies in women. Despite great advances in the treat-

ment of BRCA in recent years, tumor metastasis and recurrence rates remain persistently high and patient prognosis remains poor. TME has emerged as a pivotal determinant of tumor biology, with accumulating evidence underscoring its indispensable role in tumor progression. For instance, driving therapeutic resistance through immune suppression [7]. Notably, the precise molecular drivers and mechanistic basis underlying its functional contributions to BRCA pathogenesis remain incompletely characterized [21]. Therefore, it is important to accurately analyze the relationship between TME characteristics and clinical outcomes and to find new biomarkers for improving BRCA prognosis and improving patient survival [3].

In our study, we demonstrated that BRCA patients with elevated TME ImmuneScore exhibited significantly prolonged superior survival (log-rank $p < 0.05$). In previous studies, multiple anti-tumor mechanisms have been identified in

IGLL5 as indicator for BRCA

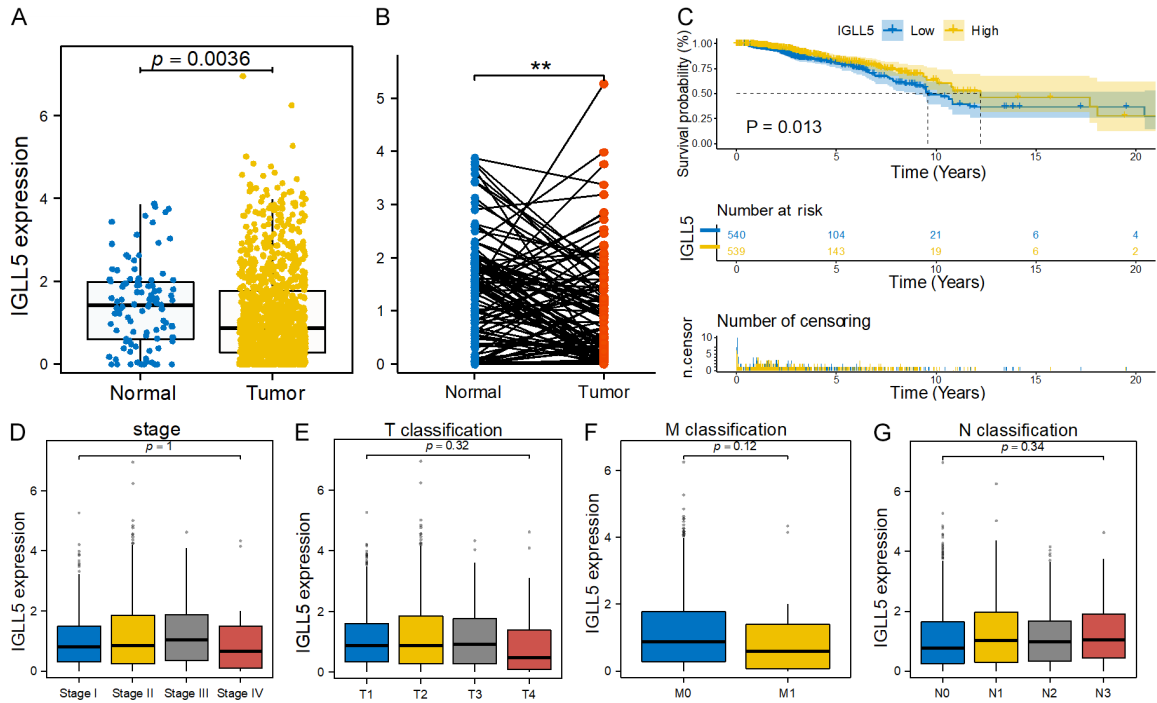


Figure 6. The differentiated expression of IGLL5 in samples and correlation with survival and clinicopathological staging characteristics of BRCA patients. A. Differentiated expression of IGLL5 in the normal and tumor sample. B. Paired differentiation analysis for expression of IGLL5 in the normal and tumor sample deriving from the same one patient. C. Survival analysis for BRCA patients with high and low IGLL5 expression ($P=0.013$, log-rank test). D-G. The correlation of IGLL5 expression with clinicopathological staging characteristics, including tumor stage, T classification, M classification, and N classification.

TME. For example, $CD8^+$ T cells recognize tumor antigens and release perforin and granzyme to directly induce apoptosis of tumor cells [22]. In addition, $IFN-\gamma$ in TME enhances antigen presentation and promotes immune surveillance [12]. These findings are consistent with our results: elevated ImmuneScore in TME correlate with prolonged survival in BRCA, whereas increased StromaScore in TME are associated with shorter survival. This phenomenon may be linked to biochemical reactions mediated by stromal components within TME. Research indicates that complex biochemical reactions within TME critically influence tumor cell survival and invasion [23]. Studies have revealed that hypoxia-induced activation of HIF-1 α in TME promotes tumor cell glycolysis, leading to lactate accumulation and subsequent facilitation of tumor cell invasion [24, 25]. Moreover, researches shown that TME and limited photosensitizer permeability critically compromise ROS-dependent therapeutic strategies in BRCA, while concurrent stromal signaling via the IL-6/STAT3-ER α axis and CXCR4/ACKR3-growth factor receptor cooperativity drives metasta-

tic progression [26, 27]. These findings collectively underscore that ImmuneScore and StromaScore within TME may play divergent roles in BRCA. Furthermore, we identified IGLL5 as a novel TME-associated risk gene, bridging stromal evolution with clinical outcomes.

IGLL5, a member of the immunoglobulin superfamily, is a key component of B cell receptor (BCR) signaling pathway and plays an important role in immune regulation. Previous studies have demonstrated that IGLL5 activation-induced by cytidine deaminase (AID) has been demonstrated to drive disease progression in hematological malignancies. These mutations induce functional aberrations that disrupt B-cell/T-cell developmental trajectories, culminating in immune surveillance evasion and clonally dominant proliferative expansion [28-30]. IGLL5, typically associated with B-cell development, promotes hematologic malignancies through BCR signaling pathway activation [28], while in solid tumors with structurally complex TME, it primarily mediates immune cell infiltration to exert pro-tumor effects.

IGLL5 as indicator for BRCA

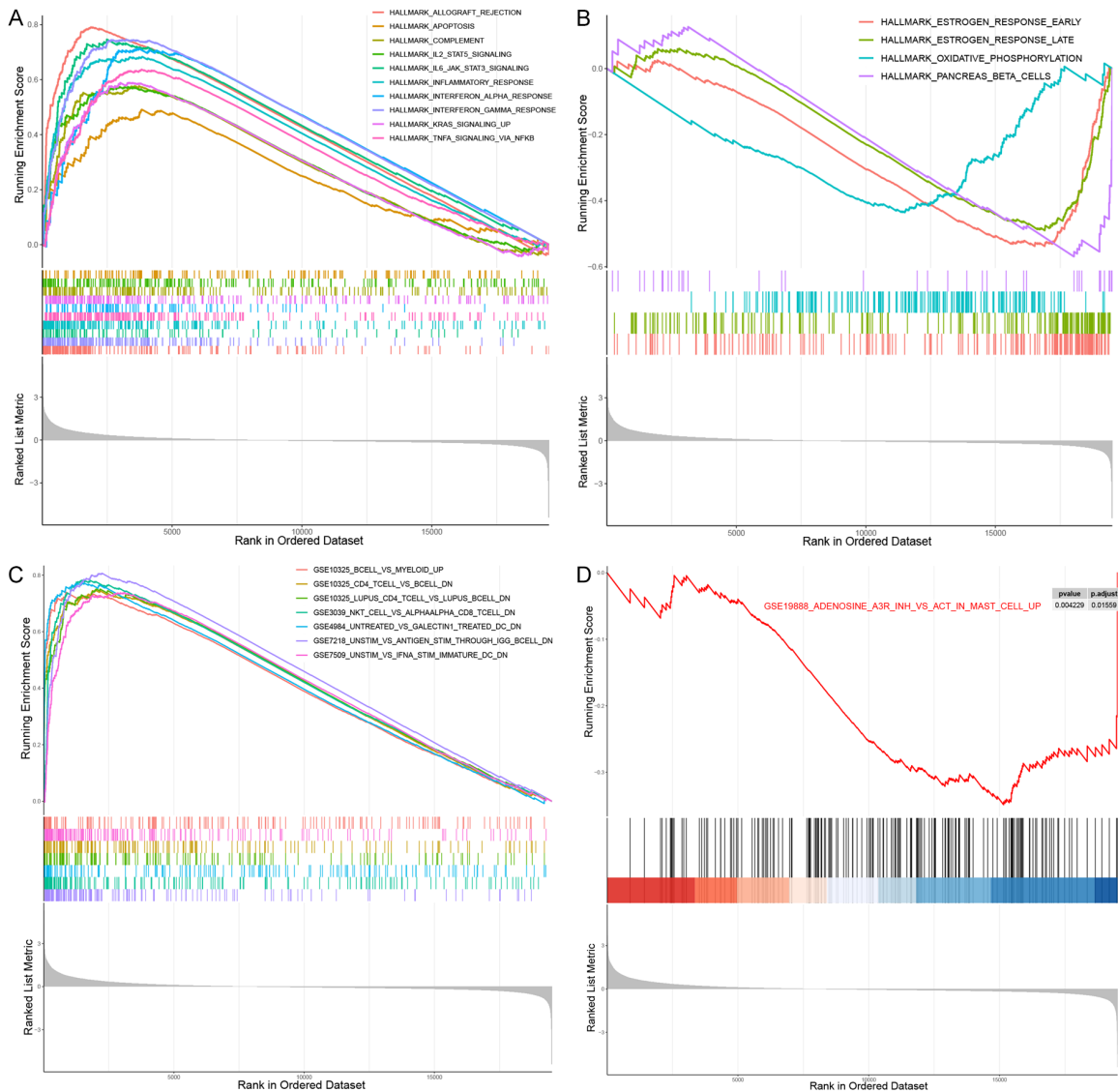
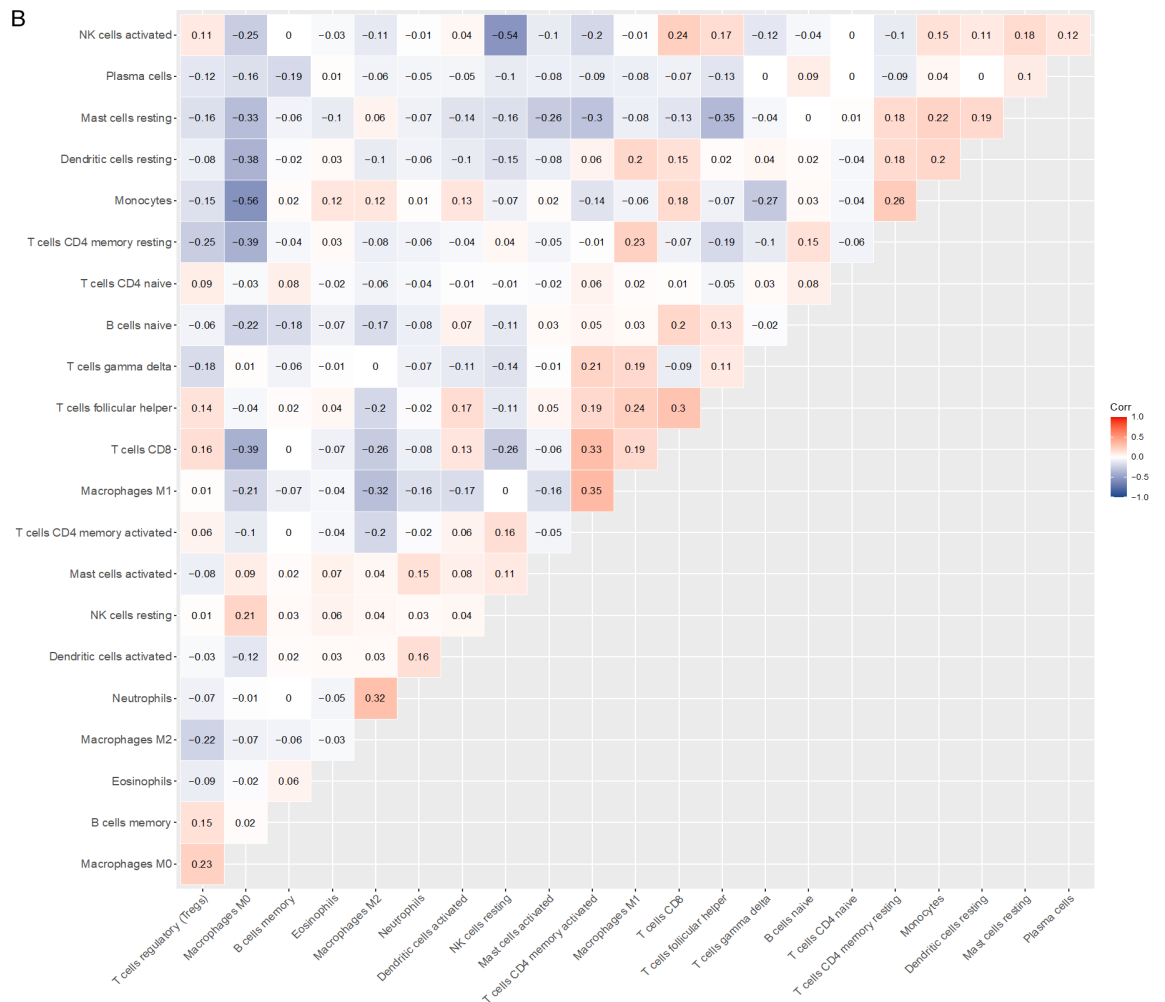
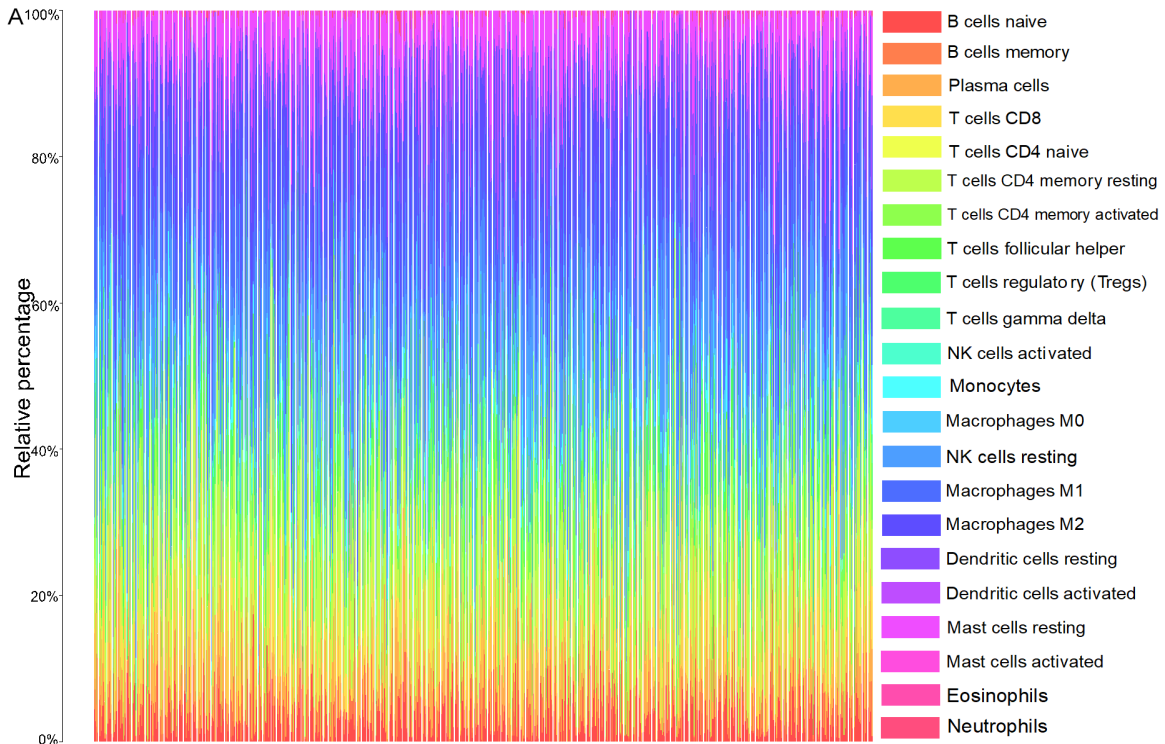


Figure 7. GSEA for samples with high IGLL5 expression and low expression. A. The enriched gene sets in HALLMARK collection by the high IGLL5 expression BRCA samples. Each line representing one particular gene set with unique color. Only gene sets with NOM $p < 0.05$ and FDR $q < 0.06$ were considered significant. B. Enriched gene sets in HALLMARK by BRCA samples with low IGLL5 expression. C. Enriched immunologic gene sets in C7 collection by high IGLL5 expression BRCA patients. D. Enriched gene sets in C7 collection by the low IGLL5 expression BRCA patients.

Our study revealed that IGLL5 exerts notable effects on complement activation, interleukin signaling, and interferon-gamma response-key immune-related pathways involved in tumorigenesis within TME. Accumulating evidence indicates that the complement system plays complex roles in TME, with its impact varying depending on tumor type and microenvironmental characteristics [31, 32]. Studies have shown that the metabolism of CD3 (+) C1q (+) tumor-associated macrophages (TAM) in TME induced by C1q signaling improves the survival prognosis of liver cancer patients [33]. Re-

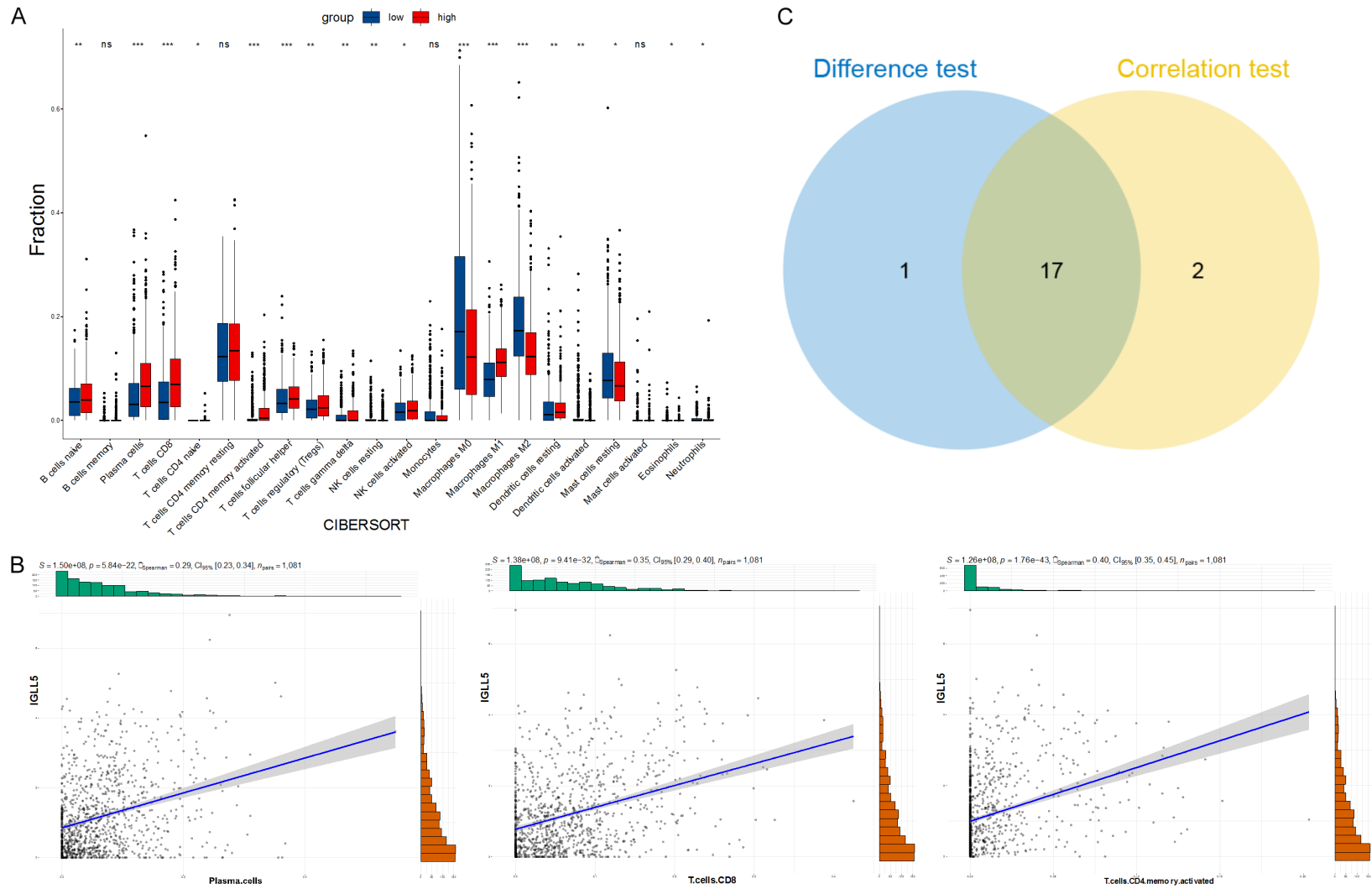
cent studies reveal the dual role of C1q in tumors, exogenous C1q exerts anti-proliferative effects on BRCA cells, whereas recombinant gC1qR promotes proliferation [34]. Nevertheless, in our research IGLL5 enhanced complement activation and improved survival rates in BRCA patients, suggesting that IGLL5 may disrupt tumor cell defense mechanisms by blocking gC1qR within TME. The interleukin network (e.g., IL-33/ST2 axis) remodels TME through immune cell recruitment, potentially mediating malignant regression [35, 36]. CAR-T cells enhance tumoricidal capacity in TME through

IGLL5 as indicator for BRCA



IGLL5 as indicator for BRCA

Figure 8. TIC profile in BRCA samples and correlation analysis. A. Barplot showing the proportion of 21 kinds of TICs in BRCA samples. Column names of plot were sample ID. B. Heatmap showing the correlation between 21 kinds of TICs and numeric in each tiny box indicating the p value of correlation between two kinds of cells.



IGLL5 as indicator for BRCA

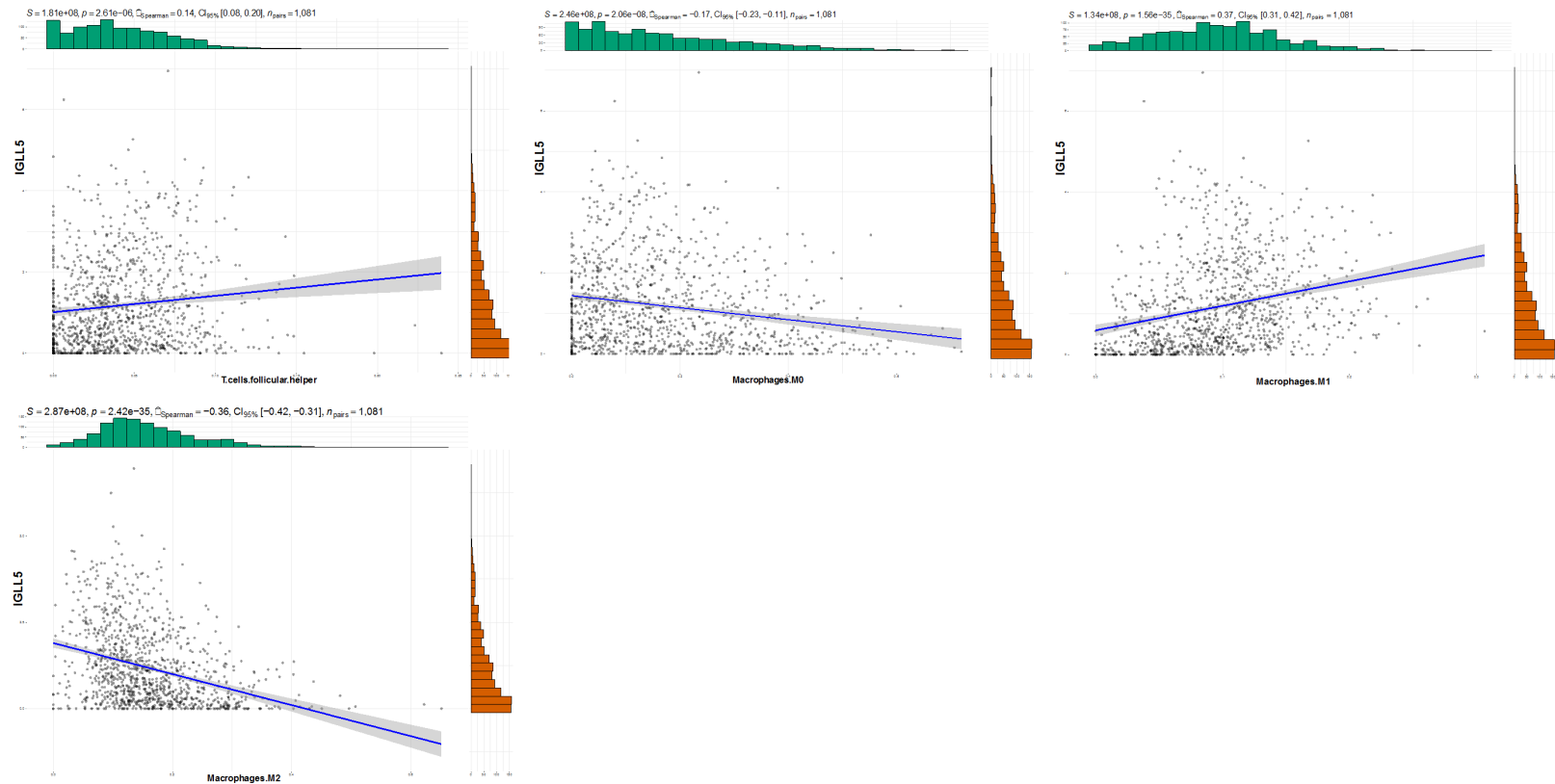


Figure 9. Correlation of TICs proportion with IGLL5 expression. A. Violin plot showed the ratio differences of 21 kinds of immune cells between BRCA samples with low or high IGLL5 expression, and Wilcoxon rank sum was used for the significance test. B. Scatter plot showed the correlation of 7 kinds of TICs proportion with the IGLL5 expression ($P < 0.001$), and Pearson coefficient was used for the correlation test. C. Venn plot displayed 17 kinds of TICs correlated with IGLL5 expression codetermined by difference and correlation tests displayed in violin and scatter plots, respectively.

interferon-gamma (IFN- γ) production, which amplifies endogenous T-cell and natural killer cell activity [37]. In our study, IGLL5 had a significant effect on interleukin signaling and interferon- γ response. These findings suggest that IGLL5 may serve as a promising indicator of immune regulation in TME, potentially influencing BRCA through modulation of immune-related pathways.

We found that IGLL5 levels positively correlate with CD8⁺ T cells. CD8⁺ T cells play a vital role in eliminating intracellular infections and malignant cells, providing long-term protective immunity [22]. Therefore, upregulation of IGLL5 may enhance immune infiltration of CD8⁺ T cells in TME by activating their effector functions, thereby promoting tumor cell killing [38]. IGLL5 expression also showed a positive correlation with plasma cell infiltration, which is known to produce local antibodies contributing to anti-tumor immunity [39]. CD38⁺ plasma cell infiltration is associated with prolonged metastasis-free survival in BRCA [40], and tumor-specific antibodies secreted by plasma cells may serve as prognostic markers in serum [41]. Although these results do not directly indicate that IGLL5 is associated with specific antibodies secreted by plasma cells, they provide valuable insights. Our research found that IGLL5 expression positively correlates with the infiltration levels of M1 macrophages and negatively with M0 and M2 macrophages. Monocytes play a crucial role in TME in BRCA. M1 macrophages are known to resist tumors, while M2 polarized macrophages, often referred to as TAMs, promote tumor progression through mechanisms such as angiogenesis and lymphangiogenesis regulation, immune suppression, hypoxia induction, tumor cell proliferation, and metastasis [42, 43]. In our study, the upregulation of IGLL5 promoted the prognosis of BRCA, suggesting that IGLL5 may enhance the phagocytosis of M1 on tumor cells and weaken the role of M2 in inducing angiogenesis in TME. These findings suggest that IGLL5 may exert an anti-tumor effect by modulating immune cell infiltration in TME, providing new insights into the targeted treatment of BRCA.

New insights into the relationship between IGLL5 expression and its prognostic value for BRCA have been provided by the current research; however, several limitations must be acknowledged. Most of the data were obtained

from online databases, which precluded access to detailed patient information and specific treatment regimens. Therefore, further rigorous experimental validation and clinical investigations are warranted to elucidate the biological functions and potential mechanisms of IGLL5 in BRCA.

In summary, it was indicated by the findings that IGLL5 expression in BRCA may play a critical role in determining disease progression and outcomes by modulating immune cell infiltration within the tumor microenvironment. A novel perspective based on IGLL5 has thereby been proposed for prognostic assessment and individualized therapeutic strategies in BRCA, with the potential to enhance clinical outcomes and survival through interventions targeting the tumor microenvironment.

Acknowledgements

We thank all the families for participating in this research project. This work was supported by National Natural Science Foundation of China (U2267220); National Natural Science Foundation of China (12405392); Youth Project of Natural Science Foundation of Jiangsu Province (BK20240358); CNNC “Young Talents” scientific research Project (Qi Ming Xing); Open Project of the State Key Laboratory of Radiation Medicine and Radiation Protection (GZK120-20042); Medical Key Laboratory of Radiation Biology and Epidemiology of Henan Province (HNRBEKF202401); Internal Cooperation Project of State Key Laboratory of Radiation Medicine and Radiation Protection (GZN1202-201); Pre-research Fund of the Second Affiliated Hospital of SU (SDFEYBS2304); and Gusu Talent Program (GSWS2022042).

Disclosure of conflict of interest

The authors state that they conducted the research without any commercial or financial relationships that could be considered a potential conflict of interest.

Address correspondence to: Huahui Bian, Department of Nuclear Accident Medical Emergency, The Second Affiliated Hospital of Soochow University, Suzhou 215004, Jiangsu, China. E-mail: bianhuahui85@163.com; Yulong Liu, Clinical Diagnosis and Treatment Center of Oncology, The Second Affiliated Hospital of Soochow University, Suzhou 215004, Jiangsu, China. E-mail: yulongliu2002@suda.edu.cn

References

- [1] Bray F, Laversanne M, Sung H, Ferlay J, Siegel RL, Soerjomataram I and Jemal A. Global cancer statistics 2022: GLOBOCAN estimates of incidence and mortality worldwide for 36 cancers in 185 countries. *CA Cancer J Clin* 2024; 74: 229-263.
- [2] Siegel RL, Giaquinto AN and Jemal A. Cancer statistics, 2024. *CA Cancer J Clin* 2024; 74: 12-49.
- [3] Waks AG and Winer EP. Breast cancer treatment: a review. *JAMA* 2019; 321: 288-300.
- [4] Veisaga ML, Ahumada M, Soriano S, Acuna L, Zhang W, Leung I, Barnum R and Barbieri MA. Anti-proliferative effect of Annona extracts on breast cancer cells. *Biocell* 2023; 47: 1835-1852.
- [5] Wu D, Chen S, Liu Y, Yang B, Li R, Jin F, Yao F and Fang Y. Single-cell analyses revealed key tumor-infiltrating myeloid cell subsets associated with clinical outcomes in different subtypes of breast cancer. *Genes Dis* 2024; 11: 101185.
- [6] Angelova M, Mlecnik B, Vasaturo A, Bindea G, Fredriksen T, Lafontaine L, Buttard B, Morgand E, Bruni D, Jouret-Mourin A, Hubert C, Kartheuser A, Humblet Y, Ceccarelli M, Syed N, Marincola FM, Bedognetti D, Van den Eynde M and Galon J. Evolution of metastases in space and time under immune selection. *Cell* 2018; 175: 751-765, e716.
- [7] Bejarano L, Jordão MJC and Joyce JA. Therapeutic targeting of the tumor microenvironment. *Cancer Discov* 2021; 11: 933-959.
- [8] White J, White MPJ, Wickremesekera A, Peng L and Gray C. The tumour microenvironment, treatment resistance and recurrence in glioblastoma. *J Transl Med* 2024; 22: 540.
- [9] Tosi A, Parisatto B, Gaffo E, Bortoluzzi S and Rosato A. A paclitaxel-hyaluronan conjugate (ONCOFID-P-B™) in patients with BCG-unresponsive carcinoma in situ of the bladder: a dynamic assessment of the tumor microenvironment. *J Exp Clin Cancer Res* 2024; 43: 109.
- [10] Gajewski TF, Schreiber H and Fu YX. Innate and adaptive immune cells in the tumor microenvironment. *Nat Immunol* 2013; 14: 1014-1022.
- [11] Denton AE, Roberts EW and Fearon DT. Stromal cells in the tumor microenvironment. *Adv Exp Med Biol* 2018; 1060: 99-114.
- [12] Zeng D, Wu J, Luo H, Li Y, Xiao J, Peng J, Ye Z, Zhou R, Yu Y, Wang G, Huang N, Wu J, Rong X, Sun L, Sun H, Qiu W, Xue Y, Bin J, Liao Y, Li N, Shi M, Kim KM and Liao W. Tumor microenvironment evaluation promotes precise checkpoint immunotherapy of advanced gastric cancer. *J Immunother Cancer* 2021; 9: e002467.
- [13] Anderson NM and Simon MC. The tumor microenvironment. *Curr Biol* 2020; 30: R921-R925.
- [14] Dvorak HF, Weaver VM, Tlsty TD and Bergers G. Tumor microenvironment and progression. *J Surg Oncol* 2011; 103: 468-474.
- [15] DeBerardinis RJ. Tumor microenvironment, metabolism, and immunotherapy. *N Engl J Med* 2020; 382: 869-871.
- [16] Thomas M, Kelly ED, Abraham J and Kruse M. Invasive lobular breast cancer: a review of pathogenesis, diagnosis, management, and future directions of early stage disease. *Semin Oncol* 2019; 46: 121-132.
- [17] Tang Q, Zhang Y, Liang Y, Qiu J, Zhang S, Jin J, Cao J, Qiao L and Feng B. The prognostic significance of FMR1 expression and its immunomodulatory implications in esophageal carcinoma. *Am J Clin Exp Immunol* 2025; 14: 14-22.
- [18] Liu S, Huang J and Zhao W. Prognosis prediction and immune microenvironment features of breast cancer indicated by a cuproptosis-associated long non-coding RNA signature. *Genes Dis* 2024; 11: 101110.
- [19] Jin J, Zhang Y, Cao J, Feng J, Liang Y, Qiao L, Feng B, Tang Q, Qiu J and Qian Z. PYG02 as a novel prognostic biomarker and its correlation with immune infiltrates in liver cancer. *Am J Clin Exp Immunol* 2025; 14: 23-33.
- [20] Qiu YU, Liu R, Huang S, Cai Q, Xie YI, He Z, Tan W and Xie X. OTUB2 promotes proliferation and metastasis of triple-negative breast cancer by deubiquitinating TRAF6. *Oncol Res* 2025; 33: 1135-1147.
- [21] Iwamoto T, Kajiwarra Y, Zhu Y and Iha S. Biomarkers of neoadjuvant/adjvant chemotherapy for breast cancer. *Chin Clin Oncol* 2020; 9: 27.
- [22] Ma X, Xiao L, Liu L, Ye L, Su P, Bi E, Wang Q, Yang M, Qian J and Yi Q. CD36-mediated ferroptosis dampens intratumoral CD8⁺ T cell effector function and impairs their antitumor ability. *Cell Metab* 2021; 33: 1001-1012, e1005.
- [23] Zhang P, Cheng S, Sheng X, Dai H, He K and Du Y. The role of autophagy in regulating metabolism in the tumor microenvironment. *Genes Dis* 2023; 10: 447-456.
- [24] Wang Y, Xiao B, Li J, Zhang M, Zhang L, Chen L, Zhang J, Chen G and Zhang W. Hypoxia regulates small extracellular vesicle biogenesis and cargo sorting through HIF-1 α /HRS signaling pathway in head and neck squamous cell carcinoma. *Cell Signal* 2025; 127: 111546.
- [25] Wei Y, Zhang D, Shi H, Qian H, Chen H, Zeng Q, Jin F, Ye Y, Ou Z, Guo M, Guo B and Chen T. PDK1 promotes breast cancer progression by enhancing the stability and transcriptional activity of HIF-1 α . *Genes Dis* 2024; 11: 101041.

IGLL5 as indicator for BRCA

- [26] Siersbæk R, Scabia V, Nagarajan S, Chernukhin I, Papachristou EK, Broome R, Johnston SJ, Joosten SEP, Green AR, Kumar S, Jones J, Omarjee S, Alvarez-Fernandez R, Glont S, Aitken SJ, Kishore K, Cheeseman D, Rakha EA, D'Santos C, Zwart W, Russell A, Brisken C and Carroll JS. IL6/STAT3 signaling hijacks estrogen receptor α enhancers to drive breast cancer metastasis. *Cancer Cell* 2020; 38: 412-423, e419.
- [27] Neves M, Marolda V, Mayor F Jr and Penela P. Crosstalk between CXCR4/ACKR3 and EGFR signaling in breast cancer cells. *Int J Mol Sci* 2022; 23: 11887.
- [28] White BS, Lanc I, O'Neal J, Gupta H, Fulton RS, Schmidt H, Fronick C, Belter EA Jr, Fiala M, King J, Ahmann GJ, DeRome M, Mardis ER, Vij R, DiPersio JF, Levy J, Auclair D and Tomasson MH. A multiple myeloma-specific capture sequencing platform discovers novel translocations and frequent, risk-associated point mutations in IGLL5. *Blood Cancer J* 2018; 8: 35.
- [29] Kasar S, Kim J, Improgo R, Tiao G, Polak P, Haradhvala N, Lawrence MS, Kiezun A, Fernandes SM, Bahl S, Sougnez C, Gabriel S, Lander ES, Kim HT, Getz G and Brown JR. Whole-genome sequencing reveals activation-induced cytidine deaminase signatures during indolent chronic lymphocytic leukaemia evolution. *Nat Commun* 2015; 6: 8866.
- [30] Pérez-Carretero C, Hernández-Sánchez M, González T, Quijada-Álamo M, Martín-Izquierdo M, Hernández-Sánchez JM, Vidal MJ, de Coca AG, Aguilar C, Vargas-Pabón M, Alonso S, Sierra M, Rubio-Martínez A, Dávila J, Díaz-Valdés JR, Queizán JA, Hernández-Rivas J, Benito R, Rodríguez-Vicente AE and Hernández-Rivas JM. Chronic lymphocytic leukemia patients with IGH translocations are characterized by a distinct genetic landscape with prognostic implications. *Int J Cancer* 2020; 147: 2780-2792.
- [31] Janneh AH, Atkinson C, Tomlinson S and Ogretmen B. Sphingolipid metabolism and complement signaling in cancer progression. *Trends Cancer* 2023; 9: 782-787.
- [32] Lei Y, Li X, Qin D, Zhang Y and Wang Y. gC1qR: a new target for cancer immunotherapy. *Front Immunol* 2023; 14: 1095943.
- [33] Yang Y, Sun L, Chen Z, Liu W, Xu Q, Liu F, Ma M, Chen Y, Lu Y, Fang H, Chen G, Shi Y and Wu D. The immune-metabolic crosstalk between CD3⁺C1q⁺TAM and CD8⁺T cells associated with relapse-free survival in HCC. *Front Immunol* 2023; 14: 1033497.
- [34] Ain D, Shaikh T, Manimala S and Ghebrehiwet B. The role of complement in the tumor microenvironment. *Fac Rev* 2021; 10: 80.
- [35] Niklander SE, Murdoch C and Hunter KD. IL-1/IL-1R signaling in head and neck cancer. *Front Oral Health* 2021; 2: 722676.
- [36] Larsen KM, Minaya MK, Vaish V and Peña MMO. The role of IL-33/ST2 pathway in tumorigenesis. *Int J Mol Sci* 2018; 19: 2676.
- [37] Boulch M, Cazaux M, Loe-Mie Y, Thibaut R, Corre B, Lemaître F, Grandjean CL, Garcia Z and Bouso P. A cross-talk between CAR T cell subsets and the tumor microenvironment is essential for sustained cytotoxic activity. *Sci Immunol* 2021; 6: eabd4344.
- [38] Farhood B, Najafi M and Mortezaee K. CD8⁺ cytotoxic T lymphocytes in cancer immunotherapy: a review. *J Cell Physiol* 2019; 234: 8509-8521.
- [39] Sharonov GV, Serebrovskaya EO, Yuzhakova DV, Britanova OV and Chudakov DM. B cells, plasma cells and antibody repertoires in the tumour microenvironment. *Nat Rev Immunol* 2020; 20: 294-307.
- [40] Heimes AS, Riedel N, Almstedt K, Krajnak S, Schwab R, Stewen K, Lebrecht A, Battista MJ, Brenner W, Hasenburger A and Schmidt M. Prognostic impact of CD38- and IgkC-positive tumor-infiltrating plasma cells in triple-negative breast cancer. *Int J Mol Sci* 2023; 24: 15219.
- [41] Rähni A, Jaago M, Sadam H, Pupina N, Pihlak A, Tuvikene J, Annuk M, Mägi A, Timmusk T, Ghaemmaghami AM and Palm K. Melanoma-specific antigen-associated antitumor antibody reactivity as an immune-related biomarker for targeted immunotherapies. *Commun Med (Lond)* 2022; 2: 48.
- [42] Boutilier AJ and ElSawa SF. Macrophage polarization states in the tumor microenvironment. *Int J Mol Sci* 2021; 22: 6995.
- [43] Song Y, Fu Y, Wang J, Tang J, Yin J, Zhang Z, Song Q and Zhang B. Complement C1q induces the M2-polarization of tumor-associated macrophages in lung adenocarcinoma. *Genes Dis* 2024; 11: 101093.